

# Evolutionary Dynamics of the Ty3/Gypsy LTR Retrotransposons in the Genome of *Anopheles gambiae*

Jose Manuel C. Tubio<sup>1,2</sup>, Marta Tojo<sup>2,3</sup>, Laia Bassaganyas<sup>1</sup>, Georgia Escaramis<sup>1</sup>, Igor V. Sharakhov<sup>4</sup>, Maria V. Sharakhova<sup>4</sup>, Cristian Tornador<sup>1</sup>, Maria F. Unger<sup>5</sup>, Horacio Naveira<sup>6</sup>, Javier Costas<sup>7</sup>, Nora J. Besansky<sup>5\*</sup>

**1** Genes and Disease Programme, Center for Genomic Regulation, Barcelona, Spain, **2** Hospital Universitario de Santiago de Compostela, Santiago de Compostela, Spain, **3** Centro Nacional de Genotipado (CEGEN), Barcelona, Spain, **4** Department of Entomology, Virginia Tech, Blacksburg, Virginia, United States of America, **5** Eck Institute for Global Health, Department of Biological Sciences, University of Notre Dame, Notre Dame, Indiana, United States of America, **6** Departamento de Biología Celular y Molecular, Universidade da Coruña, A Coruña, Spain, **7** Fundación Pública Galega de Medicina Xenómica, Complejo Hospitalario Universitario de Santiago, Santiago de Compostela, Spain

## Abstract

Ty3/gypsy elements represent one of the most abundant and diverse LTR-retrotransposon (LTRr) groups in the *Anopheles gambiae* genome, but their evolutionary dynamics have not been explored in detail. Here, we conduct an *in silico* analysis of the distribution and abundance of the full complement of 1045 copies in the updated AgamP3 assembly. Chromosomal distribution of Ty3/gypsy elements is inversely related to arm length, with densities being greatest on the X, and greater on the short versus long arms of both autosomes. Taking into account the different heterochromatic and euchromatic compartments of the genome, our data suggest that the relative abundance of Ty3/gypsy LTRs along each chromosome arm is determined mainly by the different proportions of heterochromatin, particularly pericentric heterochromatin, relative to total arm length. Additionally, the breakpoint regions of chromosomal inversion 2La appears to be a haven for LTRs. These elements are underrepresented more than 7-fold in euchromatin, where 33% of the Ty3/gypsy copies are associated with genes. The euchromatin on chromosome 3R shows a faster turnover rate of Ty3/gypsy elements, characterized by a deficit of proviral sequences and the lowest average sequence divergence of any autosomal region analyzed in this study. This probably reflects a principal role of purifying selection against insertion for the preservation of longer conserved syntenic blocks with adaptive importance located in 3R. Although some Ty3/gypsy LTRs show evidence of recent activity, an important fraction are inactive remnants of relatively ancient insertions apparently subject to genetic drift. Consistent with these computational predictions, an analysis of the occupancy rate of putatively older insertions in natural populations suggested that the degenerate copies have been fixed across the species range in this mosquito, and also are shared with the sibling species *Anopheles arabiensis*.

**Citation:** Tubio JMC, Tojo M, Bassaganyas L, Escaramis G, Sharakhov IV, et al. (2011) Evolutionary Dynamics of the Ty3/Gypsy LTR Retrotransposons in the Genome of *Anopheles gambiae*. PLoS ONE 6(1): e16328. doi:10.1371/journal.pone.0016328

**Editor:** I. King Jordan, Georgia Institute of Technology, United States of America

**Received:** September 21, 2010; **Accepted:** December 13, 2010; **Published:** January 24, 2011

**Copyright:** © 2011 Tubio et al. This is an open-access article distributed under the terms of the Creative Commons Attribution License, which permits unrestricted use, distribution, and reproduction in any medium, provided the original author and source are credited.

**Funding:** This work was supported in part by the National Institutes of Health grant AI63508 to NJB. JMCT was in part supported by a fellowship from Xunta de Galicia (Spain) and FSE European funds. No additional external funding was received for this study. The funders had no role in study design, data collection and analysis, decision to publish, or preparation of the manuscript.

**Competing Interests:** The authors have declared that no competing interests exist.

\* E-mail: nbesansk@nd.edu

## Introduction

Transposable elements (TEs) are ubiquitous components of eukaryotic genomes, but differ widely in their abundance [1]. The vast majority of these mobile elements have deleterious effects on the host genome, because of the gene mutations and chromosomal rearrangements they promote, and usually they are efficiently eliminated by selection [2]. Purifying selection acts against TEs mainly in three ways: (1) against deleterious effects of TE insertions on neighboring genes [3,4], (2) against deleterious effects of TE-generated expression products [5], and (3) against deleterious products of ectopic recombination among dispersed homologous TEs [6]. Nevertheless, each TE copy has a probability of fixation that depends not only on selective pressure, but also on host population size, and recombination frequencies in the surrounding host genomic DNA [7,8].

LTR retrotransposons (LTRrs) are TEs characterized by the presence of long terminal direct repeats (LTRs) at their ends. These elements transpose by an intracellular “copy and paste” process involving an RNA intermediate, its reverse transcription, and integration of the resulting proviral DNA. After transposition, the new proviral copies of an LTRr family are generally full-length in size and presumably active, showing no divergence at the nucleotide level from the source sequence. However, over evolutionary time it is expected that these full-length copies diverge from the template, and become fragmented due to accumulation of indels [9] and solo-LTR formation [10,11] by recombination between LTRs of the same retrotransposon.

Representative elements of the two main classes of TEs have been identified in the *An. gambiae* genome so far [12]. Recently, the comparative analysis of the genomes of the three most representative mosquitoes presented an update of their respective TE

composition [13]: in the genome of *An. gambiae*, TEs of Class II represent 5.9% of the total genome size and Class I 6.85%, of which LTRs constitutes about 2–3%. Within the LTRs, Ty3/gypsy elements comprise the most abundant and diverse group, representing 1–1.5% of the total genome size, followed by Pao/Bel (0.98%) and Ty1/copia (0.15%). Previous studies [14,15] reported that, relative to *Drosophila melanogaster* [16], the Ty3/gypsy group of *An. gambiae* is characterized by a larger proportion of degenerate copies, mainly heterochromatic. This suggested that an important fraction of Ty3/gypsy LTRr insertions have resided for a long time (as pseudogenes), leading to the prediction of high occupancy rates in the *An. gambiae* genome [14]. However, there was also evidence of recent activity by the majority of Ty3/gypsy element families in *An. gambiae*. The activity of LTRs in a genome could have important functional consequences arising not only from the transposition itself, but also from the fact that LTRs promote chromosomal rearrangements and may act as enhancers and promoters for gene transcription [3,17]. These mechanisms could be responsible for the advent of novel functions and, in the case of *An. gambiae* (one of the most important vectors of human malaria), could alter genes that contribute to epidemiologically relevant aspects of mosquito physiology or behavior, making the analysis of the associations between LTRr insertions and genes especially interesting. Here, we have performed a detailed *in silico* analysis of the patterns of distribution, abundance and occupancy of Ty3/gypsy LTRs across different structural and functional compartments of the updated *An. gambiae* genome assembly (AgamP3) [18], to yield insight into the evolutionary dynamics between these LTRs and the *An. gambiae* genome.

## Results and Discussion

### Chromosomal distribution of Ty3/gypsy LTRs

A total of 1045 insertions were identified belonging to 73 families of the Ty3/gypsy group of LTRs in the genome of *An. gambiae* (Figure 1 and Dataset S1), including 166 copies undetected in previous analyses of this group of TEs [14,15]. These insertions represent the bulk of the Ty3/gypsy complement in this genome, and constitute 1.17% of the total assembled genome size (3,197,007 bp out of 273,093,681 [19]). Each element was mapped *in silico* onto the AgamP3 assembly [18], an increase of 191 mapped insertions with respect to previous work [14,15].

Excluding the two insertions detected on the unassembled Y chromosome (the Y chromosome is entirely heterochromatic and does not polytenize), the average density of Ty3/gypsy LTRs per chromosome arm in terms of number of insertions per million bases (Mb) is 5.67 on the X and varies from 2.93 to 3.72 on the autosomes (Table 1). Taking into account that these insertions vary in size depending on their condition (i.e., fragmented or complete), the percentage of each arm composed of these LTRs is 2.0 on the X and varies from 0.64 to 1.12 on the autosomes. Thus, the X chromosome contains 17% of all the mapped insertions, despite that it comprises only 10% of the total assembled chromosome complement. These estimates are consistent with a general overrepresentation of TEs on the X chromosome of *An. gambiae* ( $\chi^2 = 36.39$ ,  $P < 0.01$ ), as reported previously for the MOZ2 [12,15] and AgamP3 [20] assemblies. In addition, autosomal density of these elements is inversely related to the size of each chromosome arm, being greater in the shorter arms 2L and 3L ( $\chi^2 = 5.08$ ,  $P = 0.02$ ).

A total of 246 Ty3/gypsy insertions (30% of the total mapped) were clustered in the genome, where clustered is defined by insertions located within 10 Kb of each other (Table 1). The pericentromeric region of the polytene complement, where

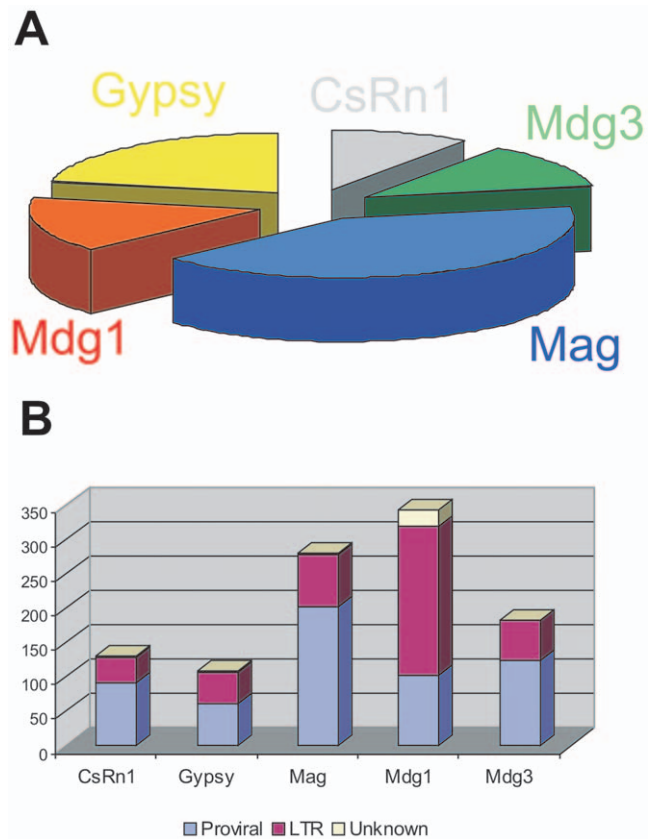


**Figure 1. The Ty3/gypsy group of LTR retrotransposons in *An. gambiae*.** The most abundant type of LTRs in the genome of *An. gambiae* is the Ty3/gypsy group, also referred to as *Metaviridae* according to virus taxonomy [51]. So far, six different lineages of this group have been identified in insects based on the phylogenetic analysis of their reverse transcriptase, ribonuclease H, and integrase amino acid domains [52,53], and designated CsRn1, Gypsy, Mag, Mdg1, Mdg3 and Osvaldo. (A) Our study in the PEST reference genome of *An. gambiae* confirmed the presence of all the insect lineages of the Ty3/gypsy group except Osvaldo, grouped in 73 well-represented families. The Mag lineage is the most diverse, presenting 41% of the total set of families, followed by Mdg3 (22%), Mdg1 (15%), Gypsy (12%) and CsRn1 (10%). (B) We analyzed a total of 1045 insertions belonging to these 73 families in *An. gambiae*. The Mdg1 lineage is the most abundant with 343 copies, most of them solo-LTRs. In the other four lineages the number of proviral copies exceeds the number of solo-LTRs. About 3% of the total amount of copies analyzed was not classified, mainly due to the presence of unsequenced gaps.

doi:10.1371/journal.pone.0016328.g001

recombination rate is lower, harbors 68% of the total copies involved in clusters. Similar findings were reported in *Drosophila* [21,22], indicating that low-recombining regions of the genome are prone to accumulation of TEs.

### Distribution and abundance of Ty3/gypsy LTRs in the heterochromatin

In terms of base pairs, the heterochromatin harbors 46% of the total mapped Ty3/gypsy complement in the genome, despite the fact that heterochromatin comprises only 7.2% of the total genome size [23]. The abundance and distribution of Ty3/gypsy LTRs was characterized relative to the three main types of heterochromatin: pericentric (PH), diffuse intercalary (DIH), and compact intercalary (CIH) [23] (Table 2, Figure 2). The PH, which represents about three quarters of total heterochromatin

**Table 1.** A comparative overview of Ty3/gypsy complement composition between chromosome arms of the AgamP3 assembly.

Arm region	LTRs sequence (bp)	% of region	Number of insertions	Insertions per Mb	Insertions in clusters	Arm size (Mb)
2L	553,250	1.12	169	3.42	64	49.36
2R	554,625	0.90	187	3.04	48	61.55
3L	428,819	1.02	156	3.72	56	41.96
3R	342,671	0.64	156	2.93	24	53.20
X	487,729	2.00	138	5.67	54	24.40
Total	2,367,094	1.03	806	3.50	246	230.47
Total <sub>UNK</sub>	3,462	-	4	-	2	0.86

For each chromosome arm column 2 shows the total base pairs of Ty3/gypsy LTRs and column 3 the % of each arm they represent. Columns 4 and 5 show the total number of insertions and the number of insertions per Mb of each region, respectively. Column 6 shows the number of insertions located 10 kb of each other. Finally, column 7 gives the total size of the chromosome region being analyzed. Last row (Total<sub>UNK</sub>) shows the information related to insertions located in euchromatin-heterochromatin intermediate regions that were not classified into the specific chromatin types showed in Tables 2 and 3.  
doi:10.1371/journal.pone.0016328.t001

size, contains 87% of the total bases of the Ty3/gypsy complement. The comparison between PH and intercalary heterochromatin (IH) shows that PH contains a higher density of Ty3/gypsy insertions (18.48 versus 14.72 insertions per Mb). This principal accumulation of insertions in the PH may result from lower rates of recombination adjacent to centromeres [24,25].

The comparison between DIH and CIH also revealed different patterns (Table 2). First, Ty3/gypsy elements comprise 6.9% of the DIH size, but only 1.6% of the CIH. Interestingly, in the latter compartment solo-LTRs are 3.7 times more abundant than proviral insertions, a significant excess relative to any other region in the genome (euchromatic or heterochromatic). Although poorly defined at the molecular level, some peculiarities of CIH have

been described. For instance, both the nuclear envelope protein lamin Dm<sub>0</sub> and the non-histone chromosomal protein HP1 bind pericentric heterochromatin, DIH, and some euchromatic regions, but not CIH [23]. Taking into account the scarce knowledge of the characteristics of CIH at the molecular level, the high proportion of solo-LTRs is difficult to interpret.

Overall, these data suggest that the relative abundance of Ty3/gypsy LTRs along each chromosome arm of *An. gambiae* is determined mainly by the different proportions of heterochromatin, particularly PH, relative to total arm length. This is especially manifest on the X chromosome where PH—accounting for 18% of the total length—contains >60% of the Ty3/gypsy insertions (Table 2).

**Table 2.** Characterization of the Ty3/gypsy complement of the AgamP3 heterochromatin.

Arm region	LTRs sequence (bp)	% of region	Number of insertions	Insertions per Mb	Proviral versus Solo-LTR	% Proviral fragmented	Average divergence	Insertions in clusters	Genes per Mb	Region size (Mb)
2L <sub>H</sub>	280,640	8.93	70	22.28	50/19	72.0	2.54±2.65	39	13.05	3.14
2L <sub>PH</sub>	232,291	9.55	56	23.03	42/13	75.0	2.41±2.53	32	12.34	2.43
2L <sub>DIH</sub>	48,349	6.81	14	19.72	8/6	57.1	3.0±3.15	7	15.49	0.71
2R <sub>H(PH)</sub>	147,873	5.77	32	12.5	25/7	47.1	2.43±2.05	13	12.11	2.56
3L <sub>H</sub>	198,661	7.69	53	20.53	32/21	69.6	2.50±2.32	34	16.65	2.59
3L <sub>PH</sub>	145,321	8.01	36	19.83	22/14	80.0	2.46±2.25	26	18.18	1.82
3L <sub>DIH</sub>	53,340	6.95	17	22.16	10/7	50.0	2.58±2.52	8	13.04	0.77
3R <sub>H</sub>	108,438	2.77	50	12.79	20/30	75.0	2.40±2.68	14	14.83	3.91
3R <sub>PH</sub>	63,439	6.11	17	16.36	13/4	81.8	1.97±2.30	5	22.14	1.04
3R <sub>CIH</sub>	44,999	1.56	33	11.49	7/26	60.0	2.76±2.99	9	12.18	2.87
X <sub>H(PH)</sub>	357,360	8.15	85	19.39	54/29	63.6	2.46±2.98	35	12.78	4.38
Total <sub>H</sub>	1,092,972	6.59	290	17.49	182/106	66.2	2.47±2.62	135	13.81	16.58
Total <sub>PH</sub>	946,284	7.74	226	18.48	157/67	68.1	2.40±2.57	111	14.15	12.23
Total <sub>DIH</sub>	101,689	6.89	31	20.99	18/13	53.3	2.79±2.80	15	14.22	1.48
Total <sub>CIH</sub>	44,999	1.56	33	11.49	7/26	60.0	2.76±2.99	9	12.18	2.87

Different heterochromatic regions were analyzed in detail: heterochromatin (H), pericentric heterochromatin (PH), diffuse intercalary heterochromatin (DIH), compact intercalary heterochromatin (CIH). Column 2 shows the total base pairs of Ty3/gypsy LTRs and column 3 the % of each arm they represent. Columns 4 and 5 show the total number of insertions and the number of insertions per Mb of each region, respectively. Column 6 gives the number of insertions of each condition category (proviral and solo-LTR), and column 7 the percentage of proviral copies that are fragmented. Column 8, the average divergence (from the consensus of the corresponding family) of the Ty3/gypsy LTRs contained in each chromosome region, and the standard deviation. Column 9, the number of insertions located within 10 Kb of each other. Column 10 gives gene density. Column 11 gives the total size of the chromosome region being analyzed.  
doi:10.1371/journal.pone.0016328.t002

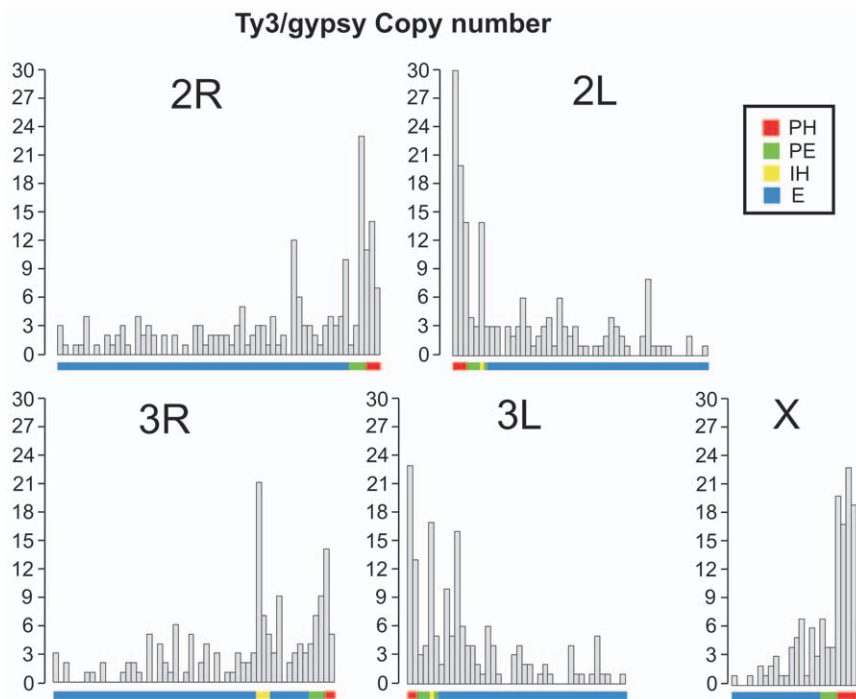


**Figure 2. Chromosomal distribution of the Ty3/gypsy complement in the AgamP3 assembly.** The distribution and relative abundance of the Ty3/gypsy insertions along chromosome arms are displayed in windows of 1 Mb. For each chromosome arm the distance from the centromere to the telomere is represented along the X axis. A coloured line under the X axis represents the different regions along each chromosome [23]: red indicates the PH; green the PE; yellow the IH; and the rest of the euchromatin is represented by a blue line. The number of insertions is represented along the left Y axis, from 0 to 30. Bars represent the abundance per Mb. See Tables 2 and 3 for details. doi:10.1371/journal.pone.0016328.g002

### Distribution and abundance of Ty3/gypsy LTRs in the euchromatin

Within the euchromatin, gene density and recombination rate are expected to play an important role in the relative abundance and distribution of the Ty3/gypsy LTRs [24,26]. Both parameters vary along each euchromatic arm, being lower adjacent to the PH [20,27,28]. Ty3/gypsy complement represents 0.6% of the total mapped euchromatin of the AgamP3 assembly (Table 3, Figure 2). As expected, the number of Ty3/gypsy insertions is greater in the pericentric euchromatin (PE) of each arm ( $\chi^2 = 87.13$ ,  $P < 0.01$ ). The PE (defined as a 3 Mb region of euchromatin proximal to the PH on each arm) represents only 7% of the total size of the euchromatic complement but it contains 17% of the total number of Ty3/gypsy euchromatic insertions. Moreover, a hotspot for Ty3/gypsy LTRs is found in the PE of 2R, where 18 insertions were clustered within a region of about 100 Kb (positions 58,001,186–58,104,526). Similar results were found for the PE of *D. melanogaster* [21,22], where the average density of LTRs is ~4-fold higher relative to the overall average in euchromatin.

As was the case for heterochromatin, the euchromatic portion of the X chromosome also contains an overrepresentation of Ty3/gypsy insertions ( $\chi^2 = 8.635$ ,  $P = 0.003$ ). Gene density does not appear to explain this significant deviation (Table 3), thus it may be due to relaxed selective pressure against LTRs in light of reduced opportunity for deleterious ectopic recombination on the X relative to autosomes in the population [2,29].

Contrary to expectation, the non-pericentromeric euchromatin (NPE) of 3R presents the lowest density of Ty3/gypsy insertions despite having the lowest gene density (Table 3). These elements represent only 0.37% of the total NPE sequence on 3R. This, together with the fact that proviral insertions in 3R present the

lowest degree of divergence among all chromosome arms (Dataset S1 and Table S1), is indicative of a faster turnover rate of proviral insertions. Interestingly, recent comparative physical mapping of congeners *An. funestus* and *An. stephensi* relative to *An. gambiae* (Sharakhova et al., unpublished data) revealed that only on 3R of *An. gambiae* are all identified syntenic blocks conserved among all three species, whereas the other autosome arms have syntenic blocks conserved only between species pairs. Lower gene density coupled with conserved microsynteny is a characteristic of genomic regulatory blocks [30]. These blocks extend over long distances and are constituted by central arrays of highly conserved non-coding elements of regulatory potential and their developmentally regulated target genes, whose maintenance is fostered by selection against the accumulation of potentially deleterious TEs [31]. In *Drosophila*, the percentage of conserved genomic sequences laying in coding regions is lower than in non-coding ones [32]. Therefore, the putative presence of genomic regulatory blocks at 3R may explain the apparent contradiction of lowest gene density coupled with lowest Ty3/gypsy insertions.

### The role of inversions on the abundance and distribution of Ty3/gypsy LTRs

The ectopic recombination model [6] suggests that the low recombination rates associated with regions adjacent to breakpoints in inversion heterozygotes [33] may reduce their deleterious effect on the host genome in those regions. Some empirical support for this model has been reported in insects, such as the 2j inversion of *D. buzzatii* [22]. Specification of the precise location of the chromosomal breakpoints for inversion 2La [34] offers an opportunity to test the potential role of inversions as shelters for TEs in *An. gambiae*. It could be predicted that the entire rearrangement (not merely the



**Table 3.** Characterization of the Ty3/gypsy complement of the AgamP3 euchromatin.

Arm region	LTRs sequence (bp)	% of region	Number of insertions	Insertions per Mb	Proviral versus Solo-LTR	% Proviral fragmented	Average divergence	Insertions in clusters	Genes per Mb	Region size (Mb)
2L <sub>E</sub>	270,776	0.59	97	2.11	56/40	30.6	2.12±2.79	25	65.26	45.90
2L <sub>PE</sub>	49,198	1.64	14	4.66	9/5	50.0	2.25±2.86	0	69.00	3.00
2L <sub>NPE</sub>	221,578	0.52	83	1.93	47/35	26.2	2.09±2.81	25	65.01	42.90
2R <sub>E</sub>	406,752	0.69	155	2.63	92/60	42.1	2.07±2.74	35	64.00	58.97
2R <sub>PE</sub>	90,482	3.02	28	9.33	19/8	66.7	3.04±3.58	19	73.33	3.00
2R <sub>NPE</sub>	316,270	0.57	127	2.27	73/52	36.9	1.91±2.58	16	63.50	55.97
3L <sub>E</sub>	229,275	0.59	102	2.60	47/48	38.1	2.08±2.62	22	53.18	39.17
3L <sub>PE</sub>	7,175	0.24	10	3.33	4/4	33.3	1.79±1.79	3	57.33	3.00
3L <sub>NPE</sub>	222,100	0.61	92	2.54	43/44	38.5	2.10±2.70	19	52.84	36.17
3R <sub>E</sub>	233,438	0.48	105	2.14	45/58	30.0	1.77±2.57	10	50.69	40.06
3R <sub>PE</sub>	34,463	1.15	23	7.66	7/16	57.1	2.42±2.48	4	34.00	3.00
3R <sub>NPE</sub>	199,025	0.43	82	1.78	38/42	24.2	1.62±2.59	6	51.78	46.06
X <sub>E</sub>	130,369	0.65	53	2.66	23/30	43.8	1.72±2.26	19	51.89	19.93
X <sub>PE</sub>	53,285	1.78	15	5.00	8/7	57.1	1.29±1.75	8	48.00	3.00
X <sub>NPE</sub>	77,084	0.46	38	2.24	15/23	33.3	1.94±2.49	11	52.57	16.93
Total <sub>E</sub>	1,270,660	0.60	512	2.40	263/236	36.8	1.99±2.65	111	58.09	213.03
Total <sub>PE</sub>	234,603	1.56	90	6.00	47/40	56.8	2.27±2.71	34	56.33	15.00
Total <sub>NPE</sub>	1,036,057	0.52	422	2.13	216/196	32.4	1.94±2.64	77	58.22	198.03

Different euchromatic regions were analyzed in detail: euchromatin (E), pericentromeric euchromatin (PE) and non-pericentromeric euchromatin (NPE). doi:10.1371/journal.pone.0016328.t003

breakpoint regions) may shelter TEs, because recombination is strongly reduced within the rearranged region in 2La/+a heterokaryotypes relative to 2La homokaryotypes, and somewhat reduced flanking the rearrangement as well [28]. The density of TEs along the 2L euchromatin (Dataset S2) was 3.08% within the limits of inversion 2La (coordinates 20,524,058–42,165,532), 5.32% between the proximal breakpoint and the pericentromeric region (coordinates 6,460,610–20,524,057), and 1.10% beyond the distal inversion breakpoint (coordinates 42,165,533–49,364,325). Although these densities differ significantly ( $P < 0.01$ ), they counter the expectation that TEs have accumulated disproportionately within the limits of the inversion. However, both 50 kb regions immediately surrounding each breakpoint contained a highly significant ( $P < 0.01$ ) increase in TE density relative to the rest of the euchromatin (13.21% and 8.53% for proximal and distal breakpoints). In addition, a 1 Mb region centered on the proximal breakpoint contained a significant increase in the number of Ty3/gypsy insertions relative to the rest of the NPE on this arm ( $\chi^2 = 13.57$ ,  $P < 0.01$ ). Similarly, the density of Ty3/gypsy LTRs is 3.3-fold higher in this 1 Mb region than the average for 2L euchromatin as a whole.

The overall data suggest that while the 2La rearrangement does not influence the overall abundance of TEs in the euchromatin of 2L, its breakpoints may do so. The role of inversions on TE distribution on chromosome 2R, where at least five rearrangements are common in complex configurations [35], remains to be investigated in detail.

### Structural variation (SV) and sequence divergence within Ty3/gypsy families

After transposition, the new copies of an LTRr family are generally full-length in size, and identical to the source sequence.

The LTRs of *An. gambiae* are typically 5 to 8 kb in length [15], and during their evolution it is expected that these full-length copies will become diverged in sequence and structure, due to solo-LTR formation and/or indel accumulation [16,21,26,36].

Assuming that consensus sequences represent full-length and active copies of the LTRr families [21], the level of divergence estimated between each copy and its family consensus provides an estimate of the age of insertion. Divergence could be estimated for 489 proviral LTRs, 239 solo-LTRs, and 10 unclassified LTRs (Dataset S1); the remaining 307 copies were excluded from the divergence analysis due to ambiguous alignments. The distribution of divergence values (Figure 3) indicates that 20% of solo-LTRs are  $\geq 99\%$  identical with their respective consensus, suggesting that solo-LTR formation [36] is an important mechanism for the inactivation of LTRr proviral insertions in their preliminary stages of evolution in the genome of this mosquito, as is the case for Ty1-like elements of the yeast *Saccharomyces cerevisiae* [10,11]. In addition, 54% of the *An. gambiae* Ty3/gypsy proviral insertions are  $\geq 99\%$  identical with the consensus, suggesting that transposition events have occurred recently in about three-quarters of the Ty3/gypsy families [15]. On the other hand, 28% of the solitary-LTRs and 11% of the proviral insertions are diverged  $\geq 5\%$  from the consensus, indicating that an important fraction of the total number of LTRs persist in the genome as pseudogenes from more ancient retroposition events.

Interestingly, the ratio of proviral to solo-LTR copies decreases with divergence (i.e., over time) (Figure 3). This suggests that selection is more efficient acting against proviral copies and/or is more permissive with solo-LTRs, given that proviral insertions are  $\sim 17$ -fold larger than solo-LTRs [15] and may be more prone to ectopic recombination [26]. Consistent with this hypothesis, Tables 2 and 3 show a significant overall preponderance of proviral insertions versus solo-LTRs in the PH relative to the NPE

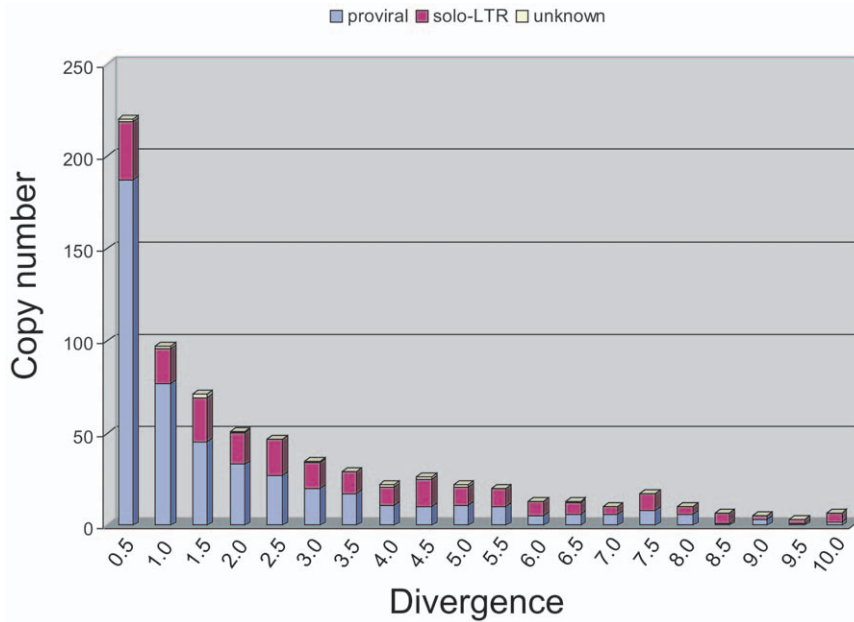


**Figure 3. Intra-family divergence of Ty3/gypsy LTRs in the genome of *An. gambiae*.** As a general rule, those copies of LTRs showing low sequence divergence from the consensus may be viewed as relatively recent transposition events in the genome, while high divergent copies may be considered remnants of older insertion events. This graph shows the relative abundance of Ty3/gypsy copies in the PEST genome relative to the divergence they present with respect to the corresponding consensus. Divergence is represented in a range from 0 to 10% in windows of 0.05. Proviral insertions are indicated in blue, solo-LTRs in red, and those unclassified (unknown) in yellow. The comparison between the group of insertions <2% divergent from the consensus, and those showing >5% divergence, reveals a significant decrease of the number of proviral copies versus solo-LTRs ( $\chi^2 = 39.00$ ,  $P \ll 0.001$ ), suggesting that selection is more efficient acting against proviral copies rather than solo-LTRs, and/or it is more permissive with solo-LTRs allowing their persistence in the genome over time. doi:10.1371/journal.pone.0016328.g003

( $\chi^2 = 18.66$ ,  $P \ll 0.001$ ), presumably because recombination is reduced and selection against proviral copies is relaxed in the PH. Moreover, there is an overall higher divergence of the insertions located in the heterochromatin versus NPE ( $t = 5.91$ ,  $P = 0.0004$ ), implying a lower turnover rate and retention of older insertions in heterochromatin, allowing genetic drift to increase the occupancy of heterochromatic insertions in populations [2,24,25].

Structural variants were classified as “partial” whenever the sum of deletion lengths exceeded 3% of the consensus sequence. A total of 905 Ty3/gypsy insertions could be classified according to this criterion (140 copies were excluded due to unreliable alignments). Approximately two-thirds of these were partial elements. Among the set of partial elements, most (73%) were solo-LTRs and the remainder were partial derivatives of proviral copies. These proviral-partial copies contribute substantially to an increase in the average divergence of the Ty3/gypsy complement (Tables 2 and 3).

More in-depth analysis of structural degradation was possible for 462 (80%) of the total proviral copies (Figure 4), of which roughly half (246) bear one or more indels  $\geq 10$  bp, and relatively few (102; 18%) are complete (i.e., without indels or unsequenced gaps). In general, the total number of deletions in an LTR copy exceeds the number of insertions (477 versus 228), as reported for *D. melanogaster* [21,26]. Accordingly, among the recent proviral copies (i.e., those  $\geq 99\%$  identical to the consensus), deletions are more frequent than insertions (63% versus 37%), being an important process for the inactivation of the proviral copies in the preliminary stages of their evolution in the genome, together with solo-LTR formation [10,11].

### Ty3/gypsy LTR retrotransposon-gene associations

The distribution of TEs along the euchromatic arms should be the outcome of both new transposition events and the strength of natural selection acting differentially against these new mutations [37] according to their location (i.e., intergenic regions, exons or introns). In the NPE of *An. gambiae*, 33% (141) of the Ty3/gypsy insertions are associated with genes (Table 4 and Table S2), similar to the observed proportion in the *D. melanogaster* genome [37]. Most genes involved in these associations are annotated as novel protein-coding and only 9% are known protein-coding genes.

Within gene boundaries, there was a significant excess of Ty3/gypsy copies located in introns. Three insertions were located in exons (Table 4), with potential functional implications. In addition, 17% of gene-associated insertions occur in the 1 kb region upstream or downstream of a gene, with potential regulatory implications [37].

For all gene-associated insertions located in the NPE, whose sequence divergence from the consensus could be estimated (114 of 141), 61% are putatively very recent (identity  $\geq 99\%$ ), suggesting that they may be polymorphic in *An. gambiae* and vary geographically among populations [38]. Most of these putatively recent insertions (83%) are proviral, consistent with the overall pattern observed in the genome (Table S1).

### Fixation of TEs in the genome

As a preliminary test of conclusions drawn from the computational analysis of Ty3/gypsy in the PEST reference genome [14,15], the level of heterozygosity (occupancy rate at an insertion site) was studied by PCR and sequencing in natural populations of *An. gambiae*. It was predicted that insertions in PEST suspected to

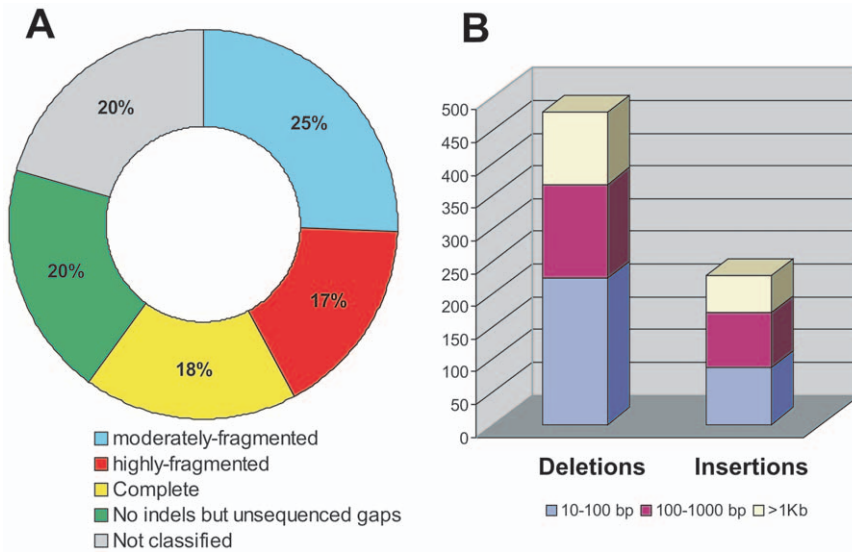


**Figure 4. Patterns of SV of the Ty3/gypsy retrotransposons of *An. gambiae*.** (A) We were able to classify 80% (462 out of 581) of the total number of proviral insertions of the Ty3/gypsy group according to their level of fragmentation (Dataset S1). The remaining 119 (20%) insertions were not classified due to unreliable alignments with respect to the respective consensus. We determined that 42% of the proviral insertions (246 out of 581) present any indel  $\geq 10$  bp: 148 (25%) are moderately-fragmented and 98 (17%) correspond to highly-fragmented insertions. On the other hand, 38% (216 out of 581) of the total number of proviral elements did not present any internal deletion or insertion  $\geq 10$  bp: 102 (18%) corresponded to true complete insertions, and the remaining 114 (20%) contain tracks of unsequenced gaps. Therefore, the total number of proviral copies with any level of fragmentation is probably underestimated. (B) We detected a total of 705 indels among the fragmented insertions of the Ty3/gypsy group of *An. gambiae*: 477 deletions and 228 insertions. Among deletions the most common are those with size in the range of 10–100 bp (47%), followed by those with size of 100 bp to 1 Kb (30%) and, finally, those longer than 1 Kb (23%). With respect to the insertions, the proportions were 38%, 37% and 25%, respectively.  
doi:10.1371/journal.pone.0016328.g004

**Table 4. Ty3/gypsy LTRr-gene associations in known protein coding genes in the PEST strain genome.**

LTRr location	Div	Condition	Proximity in bp	Gene Name	Region	Putative Gene Function
2L: 13196772–13201826	0.0	Proviral	159	MYD	5'	TOLL pathway signalling
2L: 24637421–24637824	0.7	Solo-LTR	348	CPR29	5'	cuticular protein
2L: 37133058–37136178	6.2	Proviral	0	GPRGR28	Exon	Gustatory receptor
2L: 45978291–45978633	4.5	Proviral	306	LYSC3	3'	C-type lysozyme
2L: 24637421–24637824	0.7	Solo-LTR	389	CPR28	3'	cuticular protein
2R: 4043596–4047772	0.0	Proviral	0	GPRCCK2	Intron	Putative gastrin receptor
2R: 708350–713163	0.1	Proviral	600	GPRCAL2	5'	Putative calcitonin receptor
2R: 9916959–9920921	1.0	Proviral	0	GPRALS2	Intron	Putative allatostatin receptor
2R: 9987441–9991201	0.9	Proviral	0	GPRALS2	Intron	Putative allatostatin receptor
2R: 27194388–27194533	0.0	Solo-LTR	0	CLIPD8	Intron	Clip-domain serine protease
2R: 45978291–45978633	4.5	Proviral	410	LYSC8	5'	C-type lysozyme
2R: 54126431–54126786	0.0	Solo-LTR	620	MOC2A_ANOGA	5'	Molybdenum cofactor synthesis
2R: 54126431–54126786	0.0	Solo-LTR	957	MOC2B_ANOGA	5'	Molybdenum cofactor synthesis
3L: 33267375–33267630	3.2	Solo-LTR	759	CLIPA5	3'	Clip-domain serine protease
3R: 7766729–7766729	n. d.	Solo-LTR	404	TOLL1B	5'	Toll-like Receptor
X: 6253402–6258354	0.0	Proviral	0	GPRNPY	Intron	Putative neuropeptide Y receptor
X: 7234852–1191916	0.0	Proviral	118	TPX1	5'	Thioredoxin peroxidase

We identified 17 known protein genes associated with Ty3/gypsy insertions. Column 1 gives the coordinates in the Agam P3 assembly of each insertion associated with a gene; column 2 their divergence (%) from the consensus (n. d. means “not determined”); column 3 the condition category of each insertion; and column 4 the proximity to a gene in base pairs (a proximity of 0 bp means that the insertion is located within a gene). Column 5 shows the name of the gene involved in the association. Column 6 indicates the region of the gene affected: (i) exon or intron, if the insertion is located within the transcription boundaries; and (ii) 5' and 3', if the insertion is located downstream and upstream, respectively. Column 7 shows the putative function of the gene involved in the association.  
doi:10.1371/journal.pone.0016328.t004

be relatively ancient based on high sequence divergence from the family consensus would be fixed within and among natural populations. Eight Ty3/gypsy LTRr insertion sites were initially screened with small sample sizes, and three were subsequently screened in more depth (Table S3). The initial screening was conducted by PCR, employing twenty *An. gambiae* mosquitoes (five belonged to the M and five to the S molecular forms from West Africa, and ten belonged to the S form from East Africa). This low-resolution analysis allowed us to detect at least four insertions present in all the mosquitoes sampled. Among these four, three insertions (loci *GQ468821*, *GQ468822* and *GQ468823*) were inferred to be relatively old based on their high divergence to the consensus sequence (>7% for each of the three loci). Under this hypothesis, they were subjected to more extensive population analysis with the expectation of finding high occupancy rates throughout. By comparison, the occupancy rates of four additional insertions bearing very high sequence identity with the consensus suggested that they might prove to be population-specific in larger surveys.

The presence of the three high-divergent Ty3/gypsy insertions was tested in 163 *An. gambiae* mosquitoes belonging to M and S populations from West Africa, and S populations from East Africa. In agreement with our expectations, genotyping surveys confirmed that these three insertions are present in all population samples of *An. gambiae*, showing an occupancy rate of 100%. Furthermore, we verified this observation in all the populations by sequencing of the amplicon, confirming the presence of the LTRr insertions in all the mosquitoes analyzed. The sequences of the junctions were >99% identical to the PEST reference [12] (Figure 5).

The long-term persistence of TEs in eukaryotic genomes has been explained by models of selfish DNA evolution [2]. Briefly, on the one hand natural selection is expected to put limits to the total number of elements because of their deleterious effects. On the other hand, each specific retrotransposon insertion has a low probability of fixation, which depends on selective pressure, population size, and recombination frequencies in the surrounding genome. The three fixed insertions studied showed high sequence divergence relative to the consensus, indicative of an ancient origin. Loci *GQ468821* and *GQ468823* are located in intergenic regions of the NPE of 3R and 2L, respectively. Locus *GQ468822* was not mapped onto chromosomes, being probably heterochromatic according to the composition of the region [18]. The data available suggest that these insertions had a near-neutral evolution until became fixed by genetic drift. The overall preponderance of divergent fragmented insertions in *An. gambiae* relative to *D. melanogaster* has been interpreted as consequence of a major role of genetic drift in the mosquito genome [14].

### *An. gambiae* and *An. arabiensis* share TE-loci

LTRr insertions at loci *GQ468821* and *GQ468823* are also present in *An. arabiensis* as evidenced by genotyping and confirmed by sequencing (Figures 5A and 5C) in samples from West and East Africa (10 each). With respect to the LTR insertion at locus *GQ468821*, all the *An. arabiensis* specimens analyzed showed the expected amplicon size, revealing an occupancy rate of 100% (20/20). Unfortunately, the amplification of the LTRr insertion at locus *GQ468823* in *An. arabiensis* was only successful when using primers F1 and R2, and only in a few samples. Nevertheless, successful amplification of locus *GQ468823* in some *An. arabiensis* samples allowed us to obtain the sequence of the junctions and, therefore, to certify presence of the LTRr insertion in the genome of *An. arabiensis* (Figure 5A). Thus, these results suggest that the Ty3/gypsy-like insertions common to *An. gambiae* and *An. arabiensis* transposed into the genome before the split of both species or,

alternatively, the insertions could be shared through recent genetic introgression [39]. Unfortunately, the limited data available, together with the fact that these two species have recently speciated and gene flow between them still persists, make difficult to distinguish unambiguously between introgression and the probable condition of ancestral insertions [40].

## Methods

### *In silico* identification of Ty3/gypsy insertions

The identification and family assignments of Ty3/gypsy LTRr copies were obtained following the criteria defined by Tubio et al. [15] with some refinements. Briefly, the canonical sequences of each family (or consensus sequences, when possible) were recruited from Repbase [41]. The canonical sequences represent complete copies putatively active, and the consensus sequences correspond to those constructed after alignment of at least three complete copies of each family [14,15]. BlastN searches [42] were performed, with default parameters, using as query each one of the consensus-canonical sequences of each LTRr family, providing a list of coordinates of putative LTRr copies in the genome. Next, different LTRr copies were assigned to the same family following these rules: (1) they present at least a contiguous stretch of 400 bp of the pol and/or gag region with an identity of at least 90% with the family consensus-canonical sequence; or (2) they present an identity of at least 90% over at least half of the LTR sequence length.

### *In silico* mapping of Ty3/gypsy insertions

Chromosomal locations of all the Ty3/gypsy copies in the AgamP3 assembly were obtained through the genome browser of VectorBase [19]. The recent availability of the approximate coordinates delimiting the different chromatin regions in the AgamP3 assembly [23] allowed us to determine the euchromatic type. Briefly, boundaries of PH were identified in the polytene chromosome 2 (bands 19E-20A), chromosome 3 (37D-38A), and in the X (band 6); DIH in regions of 2L (band 21A) and 3L (band 38C); and CIH in a region of 2.9 Mb of 3R (band 35B). Additionally, we defined the PE as the 3 Mb region of the euchromatin of each chromosome arm proximal to the PH, which involves euchromatic regions in 2L (coordinates 2,487,770–5,042,389 and 6,015,228–6,460,609), 2R (55,969,802–58,969,802), 3L (1,896,830–4,235,209 and 5,133,257–5,794,878), 3R (49,131,026–52,131,026), and X (16,928,574–19,928,574). Accordingly, we defined NPE as the euchromatic region of each chromosome excluding the PE. The term “pericentromeric region” refers to the chromosomal region extending from PE to PH.

### Estimation of TEs density along 2L

We used RepeatMasker (<http://www.repeatmasker.org/>) to search any trace of any known TE family in the genome of *An. gambiae* (PEST), which are those registered in RepBase [41] and TEfam (<http://tefam.biochem.vt.edu/tefam/index.php>). Then, average density of TEs was estimated as percentage of base pairs for each range of 50 Kb occupied by TEs.

### SV and divergence analyses

The SV and the divergence were estimated after alignments of each copy with the consensus sequence of the corresponding LTRr family. These alignments were performed manually, using the results of the BlastN described above as a guide, with the help of the sequence editor BioEdit version 5.0.9 [43]. In some cases, unreliable alignments were obtained avoiding a correct assessment





**Figure 5. Fixation of Ty3/gypsy insertions in *Anopheles gambiae*.** The extensive population and sequencing analyses of three highly divergent Ty3/gypsy insertions in *An. gambiae* confirmed their fixation in the species. The Gene Bank accession numbers for these loci are GQ468823, GQ468822, and GQ468821. Additionally, the presence of loci GQ468823 and GQ468821 were also confirmed in the closely related species *An. arabiensis*. This figure shows the multiple sequence alignments along the entire insertion and junctions obtained through an extensive population analysis. The DNA sequenced corresponds to mosquitoes of molecular forms M and S of *An. gambiae* from Goundry (Burkina Faso), two populations of the molecular form S from the villages of Asembo and Jogo in Kenya (AsemboS and JogoS), and two populations of *An. arabiensis* from Burkina Faso and Kenya. In addition, the corresponding sequences from the PEST strain [12] are also shown. (A) Alignment of nucleotide sequences for locus GQ468823. Sequence of the LTRr copy extends from position 15 to 314. Target site duplication (CTTAT) corresponds to positions 9–14 and 315–319. Sequences of the junctions correspond to positions 1–8 and 320–328. “b” and “f” indicate the first and last positions of the insertion, respectively. (B) Alignment of nucleotide sequences for locus GQ468822. Sequence of the LTRr copy extends from position 25 to 213. Target site duplication (CTTC) corresponds to positions 21–24 and 214–217. Sequences of the junctions correspond to positions 1–20 and 218–237. (C) Alignment of nucleotide sequences for locus GQ468821. Sequence of the LTRr copy extends from position 25 to 205. Target site duplication (CAAG) corresponds to positions 21–24 and 206–209. Sequences of the junctions correspond to positions 1–20 and 210–229.

doi:10.1371/journal.pone.0016328.g005

of their SV and/or divergence. The probable cause of these mismatches is mosaic evolution, which is known to have played an important role in the molecular evolution of Ty3/gypsy group in *An. gambiae* [14] and *Drosophila* [44].

For a description of the SV we first followed the criteria defined by Kaminker et al. [21], which considered as partial any LTRr copy less than 97% of the length of the canonical-consensus sequence of their corresponding family. Nevertheless, an important fraction of the Ty3/gypsy elements analyzed contains tracks of Ns, representing unsequenced gaps that mask the LTRr sequence, making the estimate of their length unapproachable. Therefore, we alternatively redefined the category “partial” as any LTRr copy for which the sum of the length of the deletions exceeds 3% of the length of the respective canonical-consensus sequence. Additionally, we defined two other categories that provide further information about the level of degradation of an element: (1) “moderately-fragmented”, which comprises those LTRr copies showing 1 or 2 indels  $\geq 10$  bp with respect to the consensus sequence of the corresponding LTRr family; and (2) “highly-fragmented”, which comprises those presenting  $\geq 3$  indels  $\geq 10$  bp. As a consequence, those LTRrs without indels  $\geq 10$  bp, presenting the same length as the consensus sequence of the corresponding family, were considered complete. Those insertions bearing identity exclusively to the LTR of a family consensus sequence were considered solo-LTRs. Those insertions with unsequenced gaps but meeting the criteria to be regarded as putatively complete based on the analysis of the available sequence were classified as “unknown” condition.

The divergence between each LTRr copy and the corresponding consensus was estimated as the proportion of nucleotide differences with the aid of MEGA version 2.1 [45], using the pairwise deletion option.

### Gene-LTRr association analysis and gene density estimation

We defined a gene-LTRr association as an LTRr located within the transcription borders of a gene or within 1000 bp upstream or downstream of a gene [37]. All the Ty3/gypsy LTRrs located in the NPE were submitted to this analysis. BioMart [46] was employed to identify these associations by comparison of our insertion coordinates and the gene coordinates in the AgamP3 dataset (AgamP3.5 gene set) of Ensembl [47]. Finally, we used the Ensembl genome browser to elucidate if insertions were located in an intron or exon.

Gene density was measured dividing the number of genes contained in each region and the total number of base pairs of the region. Gene content was recruited from both Ensembl and VectorBase [19,47].

### Study sites and mosquito collections

We studied populations from Kenya and Burkina Faso. In Kenya (East Africa), the study sites include: (1) Asembo Bay (in the

text referred to as Asembo), located on the shores of Lake Victoria in Western Kenya; and (2) Jogo, located 700 km away, on the coast of the Indian Ocean near the Tanzanian border. The mosquitoes belonging to molecular form S were collected from both sites in 1987 [48]. The DNA samples analyzed in this study include 46 mosquitoes from Asembo and 19 mosquitoes from Jogo. In addition, DNA samples from 10 mosquitoes of *An. arabiensis* collected in Asembo were also analyzed. Both populations, Asembo and Jogo, are separated by the Great Rift Valley, which represents a restrictive barrier to gene flow within the species *An. gambiae* [49]. In Burkina Faso (West Africa), the study site was Goundry, where mosquitoes were collected in 2001. The DNA samples analyzed include 50 mosquitoes of the species *An. gambiae* form M, 48 of *An. gambiae* form S and 10 mosquitoes of *An. arabiensis*.

### Loci selection for the occupation rate analysis

The occupation rate analysis of a set of selected insertions was carried out in order to assess the possible role of genetic drift in the evolution of divergent Ty3/gypsy insertions in the *An. gambiae* genome [14]. The selection of putative ancient insertions was prioritized as follows: first, those copies 7%–10% divergent relative to the consensus were recruited; among these divergent insertions, and to facilitate the PCR process, those displaying shorter size (i.e., 150–300 bp), and without indels and/or unsequenced gaps, were selected for the PCR optimization process. A total of 13 insertions passed these filters, although only 3 of them overcame the PCR optimization process satisfactorily (Figure S1). In addition, the occupation rate of five low divergent insertions (Table S3) without indels and unsequenced gaps (Tubio et al., unpublished data) was determined for comparisons.

### Primer design, genotyping and sequencing

In general, two different PCRs and, therefore, two different sets of primers were designed per LTRr locus selected for the occupancy rate analysis. The first set of primers, named F1 and R1 (forward1 and reverse1, respectively), were designed outside the TE copy and flanking it. For the second set of primers, named F1 and R2 (forward1 and reverse2, respectively), the reverse primer was designed inside the copy. All primers were designed with the aid of GeneFisher [50], using default parameters. PCR reactions were as follows: 0.6  $\mu$ M primer forward, 0.6  $\mu$ M primer reverse, 1.5 mM  $Mg^{+2}$ , 0.16 mM dNTPs, 1x Taq buffer and 1.25 Units of Taq polymerase were mixed in a total reaction volume of 25  $\mu$ l. The PCR cycle conditions were as follows: one cycle of 95°C for 5 min, followed by 35 cycles of 95°C for 30 sec, annealing temperature for 30 sec, 72°C for 45 sec; and finally one extension extra cycle of 72°C for 10 min. For the screening analysis, amplicons were visualized in agarose gels stained with ethidium bromide. For those three loci selected for the extensive

analysis (GQ468823, GQ468822, and GQ468821) genotyping was carried out in a 3730 Applied Biosystems sequencer, using GeneScan 500 LIZ ladder (Applied Biosystems) for a correct assignment of the amplicon size. The sequences of the primers, annealing temperatures and expected amplicons sizes are detailed in Table S4. For sequencing, the amplicons were extracted from 3% agarose electrophoresis gels and purified using QIAquick Gel Extraction Kit (Qiagen). Sequencing PCR reactions were performed using BigDye v3.0 (Applied Biosystems). Dyes were removed using an ethanol-based protocol, and PCR products were diluted in deionized formamide. Sequencing was carried out in a 3730 Applied Biosystems sequencer.

## Supporting Information

**Dataset S1 Characterization of the Ty3/gypsy complement of *An. gambiae*.** This Excel file contains information relative to the characterization of 1045 insertions of the Ty3/gypsy group in the AgamP3 assembly. Column 1 indicates the Ty3/gypsy lineage and column 2 the name of the Ty3/gypsy family [15]. Column 3 indicates the scaffold where each insertion was identified. The coordinates (first and last positions) of each insertion in a scaffold are shown in columns 4 and 5. Columns 6, 7, 8 and 9 indicate results of the *in silico* mapping: column 6 the chromosome (Chr), columns 7 and 8 the coordinates, and column 9 the cytogenetic division/subdivision. Column 10 shows the classification of each insertion according to two categories: proviral or solo-LTR (“unknown” means that classification was not possible due to the presence of unsequenced gaps). Column 11 indicates the sequence divergence (Div) from the consensus. Finally, column 12 indicates the SV relative to the consensus sequence. Three different types of SV were studied: “del” means “deletion”, “ins” means “insertion”, and “dup” means “duplication”. “No” means “no SV”. “ND” means “not determined”. SV events were annotated as follows: different SV events are separated by a comma; the size of the SV event in base pairs is indicated after each SV type; the symbols “(5’)” and “(3’)” after SV events indicate that the SV affects, respectively, the LTR5’ or LTR3’. If two different SV events occur at the same nucleotide position they are separated by a dash.  
(XLS)

**Dataset S2 TE density along chromosome 2L.** This excel file shows the density of total TEs in ranges of 50 Kb along the 2L arm. Columns 1 and 2 indicate the coordinates along the chromosome. Column 3 gives the estimation of TE density.  
(XLS)

**Table S1 Average divergence of proviral copies and solo-LTRs.** This table shows the average divergence and standard deviation of the total number of proviral and solo-LTR insertions of each chromosome for which it was possible to determine their divergence relative to the consensus. “N” indicates the number of insertions analyzed (data recruited from Dataset S1).  
(PDF)

**Table S2 Ty3/gypsy LTRr-gene associations in *An. gambiae*.** This file shows all the associations detected between Ty3/gypsy retrotransposons and genes in the *An. gambiae* genome. Column 1 indicates the chromosome where each association was detected. Columns 2 and 3 give the coordinates of each insertion associated to a gene. Column 4 indicates the classification of each insertion according to two categories: proviral and solo-LTR (“unknown” means that classification was not possible due to the

presence of unsequenced gaps). Column 5 gives the sequence divergence from the consensus. Column 6, 7 and 8 indicate the VectorBase gene identifier (AGAP number) of the associated gene and the coordinates in the genome. Column 9 shows the proximity to a gene in base pairs (proximity of 0 bp means that the insertion is located within a gene). Column 10 indicates the region of the gene affected: “exon” or “intron” if the insertion is located within transcription boundaries, and “5’” and “3’” if the insertion is located, respectively, downstream or upstream of a gene. Finally, Column 11 shows the putative function of the gene involved in the association, if known, according to Ensembl [47].  
(XLS)

**Table S3 Occupancy rate of Ty3/gypsy LTRs in *An. gambiae*.** We successfully analyzed the frequency insertion profiles of eight Ty3/gypsy LTRr loci in natural populations of *An. gambiae*. Column 1 shows the name assigned to each locus analyzed (loci 6, 7 and 8 also show Gene Bank accession numbers). Column 2 indicates the lineage and family the selected loci belong to. Column 3 gives the LTRr location by chromosomal arm, coordinates, and cytogenetic division and subdivision (number and letter in parenthesis, respectively). Column 4, the chromatin type (NPE, non-pericentromeric euchromatin; IH, intercalary heterochromatin; n. d., not determined). Column 5, the structural condition (proviral or solo-LTR). Column 6 indicates the divergence of each insertion from consensus. Last columns display information relative to the results of the occupancy rate analysis. Column 7 the type of analysis performed. Columns 8 and 9 show the occupancy rate from 0.0 to 1.0 and, in parentheses, the frequency.  
(PDF)

**Table S4 Primer sequences and PCR conditions.** This table reveals the conditions for the PCR amplification of the eight Ty3/gypsy-loci selected for the occupation rate analysis. Column 1 shows the name assigned to each locus analyzed (loci 6, 7 and 8 also show Gene Bank accession numbers). Columns 2 displays information relative to the primers employed in locus amplification (see Methods). Primers F1 of loci 6, 7 and 8 were labelled with FAM in the 5’ extreme. Column 3 shows the expected amplicon size and column 4 the annealing temperatures (T).  
(PDF)

**Figure S1 Selection of Ty3/gypsy ancient insertions for the occupation rate analysis.** This graphic shows the distribution, according to their size (Y axis) and divergence relative to consensus (X axis), of those Ty3/gypsy loci lower than 500 base pairs and without indels and unsequenced gaps. Only those insertions presenting a size of 150-300 bp and without indels of, at least, 10 bp and/or without unsequenced gaps were finally selected for PCR validation. Red dots represent loci not selected for the PCR optimization process. Yellow dots represent loci selected for the PCR optimization process, but finally discarded due to amplification difficulties. Green dots represent those putative loci selected for the occupation rate analysis (Table S3).  
(TIF)

## Acknowledgments

We thank N. F. Sagnon, C. Costantini and F. Collins, who generously shared specimens from their collections. JT thanks members of the Eck Institute for Global Health at ND, especially groups of F. H. Collins and N. J. Besansky for interesting discussions, and E. Valadé for his help during the development of this research.

## Author Contributions

Conceived and designed the experiments: JMCT NJB HN JC. Performed the experiments: JMCT MT MFU. Analyzed the data: JMCT LB GE IVS

MVS CT HN JC NJB. Contributed reagents/materials/analysis tools: JMCT MT GE LB. Wrote the paper: JMCT NJB.

## References

- Hua-Van A, Le Rouzic A, Maisonhaute C, Capy P (2005) Abundance, distribution and dynamics of retrotransposable elements and transposons: similarities and differences. *Cytogenet Genome Res* 110: 426–440.
- Charlesworth B, Sniegowski P, Stephan W (1994) The evolutionary dynamics of repetitive DNA in eukaryotes. *Nature* 371: 215–220.
- McDonald JF, Matyunina LV, Wilson S, Jordan IK, Bowen NJ, et al. (1997) LTR retrotransposons and the evolution of eukaryotic enhancers. *Genetica* 100: 3–13.
- Finnegan DJ (1992) Transposable elements. *Curr Opin Genet Dev* 2: 861–867.
- Nuzhdin SV (1999) Sure facts, speculations, and open questions about the evolution of transposable element copy number. *Genetica* 107: 129–137.
- Montgomery E, Charlesworth B, Langley CH (1987) A test for the role of natural selection in the stabilization of transposable element copy number in a population of *Drosophila melanogaster*. *Genet Res* 49: 31–41.
- Charlesworth B, Langley CH, Sniegowski PD (1997) Transposable element distributions in *Drosophila*. *Genetics* 147: 1993–1995.
- Blumenstiel JP, Hartl DL, Lozovsky ER (2002) Patterns of insertion and deletion in contrasting chromatin domains. *Mol Biol Evol* 19: 2211–2225.
- Petrov DA (2002) DNA loss and evolution of genome size in *Drosophila*. *Genetica* 115: 81–91.
- Kim JM, Vanguri S, Boeke JD, Gabriel A, Voytas DF (1998) Transposable elements and genome organization: a comprehensive survey of retrotransposons revealed by the complete *Saccharomyces cerevisiae* genome sequence. *Genome Res* 8: 464–478.
- Jordan IK, McDonald JF (1999) The role of interelement selection in *Saccharomyces cerevisiae* Ty element evolution. *J Mol Evol* 49: 352–357.
- Holt RA, Subramanian GM, Halpern A, Sutton GG, Charlab R, et al. (2002) The genome sequence of the malaria mosquito *Anopheles gambiae*. *Science* 298: 129–149.
- Arensburger P, Megy K, Waterhouse RM, Abrudan J, Amedeo P, et al. (2010) Sequencing of *Culex quinquefasciatus* establishes a platform for mosquito comparative genomics. *Science* 330: 86–88.
- Tubio JM, Costas JC, Naveira HF (2004) Evolution of the mdg1 lineage of the Ty3/gypsy group of LTR retrotransposons in *Anopheles gambiae*. *Gene* 330: 123–131.
- Tubio JM, Naveira H, Costas J (2005) Structural and evolutionary analyses of the Ty3/gypsy group of LTR retrotransposons in the genome of *Anopheles gambiae*. *Mol Biol Evol* 22: 29–39.
- Lerat E, Rizzon C, Biemont C (2003) Sequence divergence within transposable element families in the *Drosophila melanogaster* genome. *Genome Res* 13: 1889–1896.
- Kidwell MG, Lisch DR (2001) Perspective: transposable elements, parasitic DNA, and genome evolution. *Evolution* 55: 1–24.
- Sharakhova MV, Hammond MP, Lobo NF, Krzywinski J, Unger MF, et al. (2007) Update of the *Anopheles gambiae* PEST genome assembly. *Genome Biol* 8: R5.
- Lawson D, Arensburger P, Atkinson P, Besansky NJ, Bruggner RV, et al. (2009) VectorBase: a data resource for invertebrate vector genomics. *Nucleic Acids Res* 37: D583–587.
- Xia A, Sharakhova MV, Leman SC, Tu Z, Bailey JA, et al. (2010) Genome landscape and evolutionary plasticity of chromosomes in malaria mosquitoes. *PLoS One* 5: e10592.
- Kaminker JS, Bergman CM, Kronmiller B, Carlson J, Svirskas R, et al. (2002) The transposable elements of the *Drosophila melanogaster* euchromatin: a genomics perspective. *Genome Biol* 3: RESEARCH0084.
- Caceres M, Puig M, Ruiz A (2001) Molecular characterization of two natural hotspots in the *Drosophila buzzatii* genome induced by transposon insertions. *Genome Res* 11: 1353–1364.
- Sharakhova MV, George P, Brusenstova IV, Leman SC, Bailey JA, et al. (2010) Genome mapping and characterization of the *Anopheles gambiae* heterochromatin. *BMC Genomics* 11: 459.
- Maside X, Assimacopoulos S, Charlesworth B (2005) Fixation of transposable elements in the *Drosophila melanogaster* genome. *Genet Res* 85: 195–203.
- Bartolome C, Maside X (2004) The lack of recombination drives the fixation of transposable elements on the fourth chromosome of *Drosophila melanogaster*. *Genet Res* 83: 91–100.
- Petrov DA, Aminetzach YT, Davis JC, Bensasson D, Hirsh AE (2003) Size matters: non-LTR retrotransposable elements and ectopic recombination in *Drosophila*. *Mol Biol Evol* 20: 880–892.
- Pombi M, Stump AD, Della Torre A, Besansky NJ (2006) Variation in recombination rate across the X chromosome of *Anopheles gambiae*. *Am J Trop Med Hyg* 75: 901–903.
- Stump AD, Pombi M, Goeddel L, Ribeiro JM, Wilder JA, et al. (2007) Genetic exchange in 2La inversion heterokaryotypes of *Anopheles gambiae*. *Insect Mol Biol* 16: 703–709.
- Charlesworth B, Langley CH (1989) The population genetics of *Drosophila* transposable elements. *Annu Rev Genet* 23: 251–287.
- Engstrom PG, Ho Sui SJ, Drivenes O, Becker TS, Lenhard B (2007) Genomic regulatory blocks underlie extensive microsynteny conservation in insects. *Genome Res* 17: 1898–1908.
- Hurst LD, Pal C, Lercher MJ (2004) The evolutionary dynamics of eukaryotic gene order. *Nat Rev Genet* 5: 299–310.
- Siepel A, Bejerano G, Pedersen JS, Hinrichs AS, Hou M, et al. (2005) Evolutionarily conserved elements in vertebrate, insect, worm, and yeast genomes. *Genome Res* 15: 1034–1050.
- Navarro A, Betran E, Barbadilla A, Ruiz A (1997) Recombination and gene flux caused by gene conversion and crossing over in inversion heterokaryotypes. *Genetics* 146: 695–709.
- Sharakhov IV, White BJ, Sharakhova MV, Kayondo J, Lobo NF, et al. (2006) Breakpoint structure reveals the unique origin of an interspecific chromosomal inversion (2La) in the *Anopheles gambiae* complex. *Proc Natl Acad Sci U S A* 103: 6258–6262.
- Coluzzi M, Sabatini A, della Torre A, Di Deco MA, Petrarca V (2002) A polytene chromosome analysis of the *Anopheles gambiae* species complex. *Science* 298: 1415–1418.
- Jordan IK, McDonald JF (1999) Comparative genomics and evolutionary dynamics of *Saccharomyces cerevisiae* Ty elements. *Genetica* 107: 3–13.
- Ganko EW, Greene CS, Lewis JA, Bhattacharjee V, McDonald JF (2006) LTR retrotransposon-gene associations in *Drosophila melanogaster*. *J Mol Evol* 62: 111–120.
- Franchini LF, Ganko EW, McDonald JF (2004) Retrotransposon-gene associations are widespread among *D. melanogaster* populations. *Mol Biol Evol* 21: 1323–1331.
- Besansky NJ, Krzywinski J, Lehmann T, Simard F, Kern M, et al. (2003) Semipermeable species boundaries between *Anopheles gambiae* and *Anopheles arabiensis*: evidence from multilocus DNA sequence variation. *Proc Natl Acad Sci U S A* 100: 10818–10823.
- Donnelly MJ, Pinto J, Girod R, Besansky NJ, Lehmann T (2004) Revisiting the role of introgression vs shared ancestral polymorphisms as key processes shaping genetic diversity in the recently separated sibling species of the *Anopheles gambiae* complex. *Heredity* 92: 61–68.
- Jurka J, Kapitonov VV, Pavlicek A, Klonowski P, Kohany O, et al. (2005) Repbase Update, a database of eukaryotic repetitive elements. *Cytogenet Genome Res* 110: 462–467.
- Altschul SF, Madden TL, Schaffer AA, Zhang J, Zhang Z, et al. (1997) Gapped BLAST and PSI-BLAST: a new generation of protein database search programs. *Nucleic Acids Res* 25: 3389–3402.
- Hall TA (1999) BioEdit: a user-friendly biological sequence alignment editor and analysis program for Windows 95/98/NT. *Nucl Acids Symp Ser* 41: 95–98.
- Costas J, Valade E, Naveira H (2001) Structural features of the mdg1 lineage of the Ty3/gypsy group of LTR retrotransposons inferred from the phylogenetic analyses of its open reading frames. *J Mol Evol* 53: 165–171.
- Kumar S, Nei M, Dudley J, Tamura K (2008) MEGA: a biologist-centric software for evolutionary analysis of DNA and protein sequences. *Brief Bioinform* 9: 299–306.
- Haider S, Ballester B, Smedley D, Zhang J, Rice P, et al. (2009) BioMart Central Portal—unified access to biological data. *Nucleic Acids Res* 37: W23–27.
- Hubbard TJ, Aken BL, Ayling S, Ballester B, Beal K, et al. (2009) Ensembl 2009. *Nucleic Acids Res* 37: D690–697.
- McLain DK, Collins FH, Brandling-Bennett AD, Were JB (1989) Microgeographic variation in rDNA intergenic spacers of *Anopheles gambiae* in western Kenya. *Heredity* 62 (Pt 2): 257–264.
- Lehmann T, Blackston CR, Besansky NJ, Escalante AA, Collins FH, et al. (2000) The Rift Valley complex as a barrier to gene flow for *Anopheles gambiae* in Kenya: the mtDNA perspective. *J Hered* 91: 165–168.
- Giegerich R, Meyer F, Schleiermacher C (1996) GeneFisher—software support for the detection of postulated genes. *Proc Int Conf Intell Syst Mol Biol* 4: 68–77.
- Boeke JD, Eickbush TH, Sandmeyer SB, Voytas DF (1998) Virus taxonomy: ICTV VIIth Report. New York: Springer-Verlag. Ed.
- Malik HS, Eickbush TH (1999) Modular evolution of the integrase domain in the Ty3/Gypsy class of LTR retrotransposons. *J Virol* 73: 5186–5190.
- Bae YA, Moon SY, Kong Y, Cho SY, Rhyu MG (2001) CsRn1, a novel active retrotransposon in a parasitic trematode, *Clonorchis sinensis*, discloses a new phylogenetic clade of Ty3/gypsy-like LTR retrotransposons. *Mol Biol Evol* 18: 1474–1483.